OPEN ACCESS Freely available online

Journal of Physical Chemistry & Biophysics

Research Article

A Non-Thermal Plasma Synergized Supported by Catalytic Investigation and Computational Analysis of the Degradation Mechanism of Chloro Containing Volatile Organic Compounds

Rajesh Kumar Mahanta, Pranita Panda, Smrutiprava Das*

Department of Chemistry, Plasma Research Laboratory, Ravenshaw University, Cuttcak, India

ABSTRACT

Volatile Organic Compounds (VOCs), particularly the chlorine containing organic compounds, are regarded as the most dangerous pollutants due to qualities such as toxicity, carcinogenicity, diffusivity, and volatility, which have a negative impact on human health and the environment. Abatement of Cl group containing VOCs to less hazardous and industrially usable compounds is a unique way to reducing VOC related concerns. Non Thermal Plasma (NTP) assisted catalysis is the ideal technology for the efficient abatement of Cl VOCs because it is more selective, energy efficient, and requires no solvent at relatively mild circumstances than other degrading methods. For this work, we chose three distinct chloro-containing gaseous pollutants, such as chlorobenzene, O-Dichlorobenzene, and dichloromethane, to assess their efficiency and mechanism with respect to catalyst by a coaxial DBD reactor. Degraded products are discovered and evaluated using GC, GCMS, FTIR, and OES. Gaussian 16 W software's computational work assisted in determining the most viable degradation pathway from among various options. Dichloromethane is more efficient than other VOCs such as chlorobenzene and o-dichlorobenzene, both with and without catalyst. MnO_2 and CeO_2 catalysts are utilized for the above VOCs, and MnO_2 has higher efficiency than CeO_2 (analyzed using XRD and FESEM graphs), resulting in increased degradation efficiency for the above compounds. The deposited products are oxidized in the plasma reactor, and with catalytic assistance, many harmful helpful compounds are generated, while harmful products are transformed into CO_2, CO, H_2O, and other useful hydrocarbons. Finally, a look at future problems and scope in the development of NTP-assisted VOC catalytic.

Keywords: NTP (Non-thermal Plasma); Co-axial DBD reactor; Gaseous pollutants (VOCs); OES (Optical Emission Spectroscopy); GCMS (Gas Chromatography Mass Spectrometry); Gaussian analysis

GRAPHICAL ABSTRACT

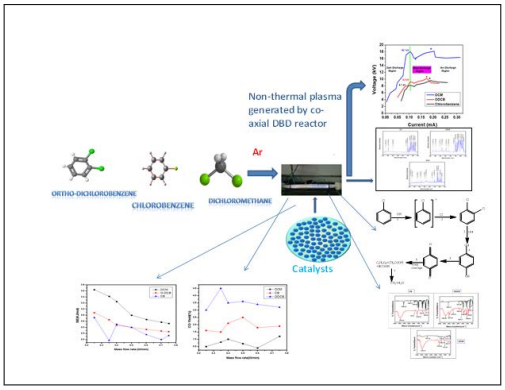

Correspondence to: Smrutiprava Das, Department of Chemistry, Plasma Research Laboratory, Ravenshaw University, Cuttcak, India, Tel: + 07978718227; E-mail: dassmrutiprava@yahoo.co.in

Received: 22-Jul-2024, Manuscript No. JPCB-24-33097; **Editor assigned:** 24-Jul-2024, PreQC No. JPCB-24-33097 (PQ); **Reviewed:** 08-Aug-2024, QC No. JPCB-24-33097; **Revised:** 27-Sep-2024, Manuscript No. JPCB-24-33097 (R); **Published:** 02-Dec-2024, DOI: 10.35841/2161-0398.24.14.411

Citation: Mahanta RK, Panda P, Das S (2024) A Non-Thermal Plasma Synergized Supported by Catalytic Investigation and Computational Analysis of the Degradation Mechanism of Chloro Containing Volatile Organic Compounds. J Phys Chem Biophys. 14:411.

INTRODUCTION

Volatile Organic Compounds (VOCs) are harmful organic pollutants that are frequently used and created by transportation, household appliances, domestic activities, and numerous industries [1-3]. Chlorinated Volatile Organic Compounds (Cl-VOCs) are employed as solvents in industry for operations such as metal degreasing, pharmaceutical production, and adhesive manufacturing [4]. Most Cl-VOCs, such as chlorobenzene, dichlorobenzene, dichloromethane, tetra chloromethane, and others, are recognized as major contributors to global air and water pollution because they are major precursors of ozone and secondary aerosols [5], photochemical smog [6], and secondary aerosols [7]. With the growing environmental degradation scenario and the widespread use of chemicals as solvents becoming a great challenge for industries and research communities that how to remove effectively Cl-VOCs without generating toxic chemicals and secondary pollutants. Compounds as solvents are posing a significant challenge to companies and research groups in terms of properly removing Cl-VOCs without emitting harmful compounds or secondary pollutants.

Cl-VOC elimination control methods include advanced oxidation, adsorption, and catalytic decomposition [8-13]. All of the following approaches are successful at removing Cl-VOCs, however they all have drawbacks in terms of efficiency and bi-product removal. Non-Thermal Plasma (NTP) is a promising technology that comprises of electrons, ions, radicals, excited species, and neutral species [14]. The excited/radical particles are analyzed *via* optical emission. Spectra are capable of breaking bonds or converting toxic compounds into less dangerous molecules [15]. The generation of ions, electrons, and reactive species such O_2^+, O_2^-, O_3^-, H_3O^+, N_2^+, and OH radicals facilitates the degradation process. These species have the ability to disrupt chemical bonds, causing contaminants in the environment to oxidize. Because of its non-equilibrium character, lack of solvent use, low energy cost, high degradation rate, ease of operation, and unique ability to initiate reaction at lower temperatures, NTP assisted catalysis is regarded as a superior alternative degradation method to conventional thermal activated catalysis.

For this project, a parallel plate DBD discharge reactor was used because it produces homogenous plasma with a high density even at low duty cycles. Owing to the aforementioned characteristics of DBD, it is employed as a possibly improved system in a variety of industries and research facilities. A review of the literature reveals that in the NTP catalyzed DBD system, removal efficiency increases, more useful products are formed, and bi-products are formed less frequently [16,17]. The degradation of chlorobenzene using plasma produced by contact glow discharge electrolysis took nearly 240 minutes to complete, indicating a longer removal process. A glow discharge was used by Chen et al. [14].

All plasma induced chemical reactions happened in the reactor, and a small amount of bi-products were deposited on the reactor's surface, which was used for study and prediction of degradation mechanism. Pulsed AC Plasma processes rely heavily on the power supply system. Chemical processes have also been shown to react differently depending on the power supply system. In this study, we used three VOCs: Chlorobenzene, ortho-dichlorobenzene, and dichloromethane to achieve maximal degradation, greater removal efficiency, comparative investigation, and computational work. We attempted to degrade the above VOCs at varied concentrations. Analyze the effect and mechanism of the above electron-drawing group, and complete the computational task. DBD is utilized for the degradation of these pollutants to get better outcomes because it has a wide range of applications, including ozone formation, material characterization, and biological ones. Various diagnostics, such as FTIR spectroscopy, GC, GCMS, and OES, are used to identify byproducts.

MATERIALS AND METHODS

Experimental

Chlorobenzene (M_W=112.56 g/mol, boiling point=131°C, purity=98%), ortho-dichlorobenzene (M_W=0147.01 g/mol, boiling point=180.19°C, purity=99%), dichloromethane (M_W=84.93 g/mol, boiling point=39.6°C, purity=99%) and catalysts were purchased from MERK India. Ethyl alcohol are purchased from local distributor. All other materials are used without any further purification.

Experimental setup

The non-thermal plasma approach is implemented using a coaxial plasma dielectric barrier discharge reactor. The schematic experimental diagram is provided in Figure 1. A 5-7 ml sample of each VOC was collected in a liquid sample container and combined with a stream of Argon, which served as a carrier gas for the abatement process. The Ar gas transports the sample into the plasma reactor and generates plasma. For this experiment, Ar gas was chosen due to its inert nature and ability to generate plasma uniformly in the DBD reactor, which aids in the breakdown of VOCs and produces better results than other gases, as well as the creation of excited species. The gas flow rate was varied between 0.20 and 0.50 lit/min, which is observed in a Mass Flow Controller (MFC) is attached to the reactor body. A high voltage pulsed power AC supply (0-10 kV with frequency 10 kHz, 20 KV p-p pulser hydrophenac firm plasma pulse technology) was linked to the DBD reactor. Plasma treated samples were collected through an airtight Teflon tube located near the reactor's exit. The input voltage for decomposition ranges from 7 kV to 22 kV at 50 Hz (7.3 to 12.4 kV for CB, 7.5 to 15.3 kV for ODCB, and 17.1 to 21.2 kV for DCM). The current was measured with a current probe (TCP0030, 158Tektronix, USA). V-Q waveforms were captured 160 times on a digital oscilloscope (DPO3012, Tektronix, USA). The plasma injected energy by cycle Specific Input Energy (SIE, J/L) was computed, allowing the calculation of the specific input energy in the reactor as follows:

The discharge Power (P) was calculated by a four channel digital oscilloscope. And from this discharge power we were able to calculate SIE (J/l) by using the formula:

$P=f\int I \times V \times t$

Where,

P=Discharge Power (Watt)∫×

F=Frequency (kHz)

I=Current (Ampere)

V=Voltage (kV)

t=Time of the pulse (sec)

The power was calculated on the basis of 12-20 oscilloscopic measurements of the current and voltage:

$SE=(P \times 0.06)/(\text{Flow rate})$

Here,

SE=Specific Energy in KJ/mol

P=Power (J/S)

Flow rate in lit/sec

The optimized condition for all these VOC decomposition is shown in a Table 1 below.

Table 1: Plasma parameters for optimization.

S. no.	VOCs	Feeding gas	Gas flow rate (LPM)	Operating Voltage (kV)	Current (A)	Power (W)	Time (min)	Freq. and duty cycle
1	Chlorobenzene	Ar	1	7.3-12.4	0.30-0.71	1.15-3.11	5	10 kHz, 20%
2	Orthodichlorobenzene	Ar	1	7.5-15.3	0.25-0.81	0.72-2.53	5	
3	Dichloromethane	Ar	1	17.1-21.2	0.26-0.90	0.91-2.75	5	

In the above case the SIE range varies from 1500-3650 J/l (1500-2750 J/l for CB, 2300-2900 J/l for ODCB and 2600-3750 J/l for DCM). The concentrations of CO_2, CO, hydrocarbons, and other compounds were determined using a Gas Chromatography (7809 B GC systems; Agilent Technologies) with a Flame Ionization Detector (FID). Gas chromatography mass spectrometry (GC, 7809 B GC equipment coupled with 5977A MSD; Agilent technology) was used to analyze by-products in both gaseous and surface deposited products. The surface deposited products were then examined using GCMS and an infrared spectrophotometer.

The concentration of VOCs is determined using a Gas Chromatography (GC 2010) with FID. The intake and output gaseous compositions are evaluated online using Fourier Transform Infrared Spectroscopy (FTIR, Nicolet 6700) and a 2.4 m gas cell. A gas chromatography (7809 B GC systems; Agilent Technologies) with a reformer furnace equipment is utilized to quantify the concentration of CO and CO_2. The organic aerosol and exhaust gas samples are evaluated qualitatively using a gas chromatography fitted with a mass detector (GC-MS, 5977A MSD; Agilent Technology) and a capillary column (HP-5MS, 30 m × 250 μm × 0.25 μm). The column temperature begins at 60°C and remains there for 2 minutes before increasing to 300°C at a rate of 10°C per minute for 3 minutes. The MS detector operates in scan mode, with a mass range of 30-600 m/z.

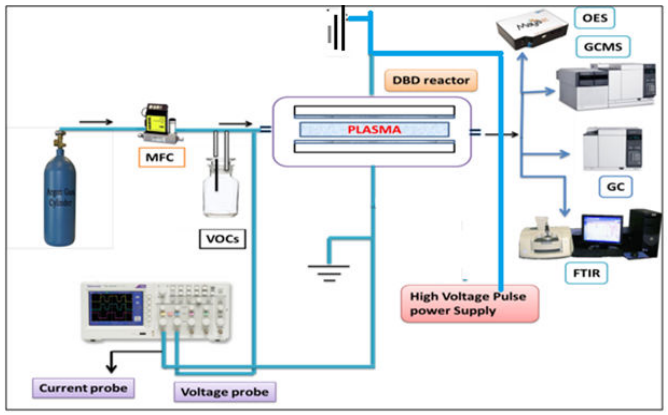

Figure 1: Schematic diagram of plasma DBD reactor.

Optimization of the plasma reactor

Optical Emission Spectroscopy (OES): Optical emission spectroscopy (USB MAYA) is a key technique for detecting reactive and energetic particles in the plasma environment. In terms of wavelength, the energetic free radicals revealed their various emission intensities that were present in the plasma environment, which was detected using NIST online data. This approach measures electronic spectra in the UV-VISIBLE range. Calculated plasma parameters provide an excellent explanation for the degradation process of these contaminants [18].

Catalyst characterization

X-ray Diffraction Method (XRD): Powder X-Ray Diffraction (XRD) patterns were recorded on RIGAKU ULTIMA-IV X-ray Diffractometer with Cu K radiation (λ=1.5418 Å) operated at 40 kV and 40 mA. AMO was further analyzed using an XTRA *in situ* X-ray diffractometer (Cu K× radiation) equipped with an Anton Paar XRK 900 heater chamber from room temperature to 450°C (under air) or 500°C (under He) at a ramping rate of 10°C min^{-1} and at 1.4 s $step^{-1}$. Diffraction patterns were obtained in the range of 50-40° at a scan rate of 3° min.

BET measurements

Specific surface area values were determined by BET method from nitrogen adsorption at liquid nitrogen temperature, using a Micromeritics Instrument Corp. FlowSorb 2300. Prior to the measurement, the samples were heated at 250°C in an inert atmosphere to clean the surface.

Morphological study

Field Emission Scanning Electron Microscopy (FESEM): Morphological studies were carried out using a Zeiss DSM 982 Gemini field emission scanning electron microscope with a Schottky emitter operating at 2.0 kv with a beam current of 1.0 mA.

Optical Emission Spectroscopy (OES): Optical emission spectroscopy (USB MAYA) is an important tool to detect the reactive and energized particles in the plasma environment. With regard to the wavelength, the energetic free radicals displayed their respective emission intensities that were present during the plasma environment and it was detected through NIST online data.

Gas Chromatography (GC): Gas chromatographic technique is used to analyse all the gaseous bi-products and GC is connected with FID column. Flame Ionization Detector (FID) detects organic compounds and its maximum temperature was up to 450°C. Nitrogen gas taken as the carrier gas along with air and hydrogen gas. Mixture of standard gases which are calibrated like CO_2, CH_4 and CO (452 ppm, 470 ppm and 450 ppm respectively purchased from Eurasian associates) are taken in GC and their respective Retention Times (RT) at 2.141, 9.921 and 11.999 minutes are checked.

Gas Chromatography Mass Spectrometry (GC-MS): Gas Chromatography Mass Spectrometry (GC-MS) is used for analysis of both gaseous and surface deposited products through a HP 5 capillary column, using Helium (He) as the carrier gas at a flow rate of 20 sccm. The peak area before and after plasma treatment at the same RT is also studied through GC-MS. From this instrument we get fragmented products of treated substances.

FTIR: The bi-products which are deposited on dielectric material are collected and washed with ethanol solution, then analysed in Fourier Transform Infrared (FTIR, thermo Fischer) spectrophotometer in the wave length range of 4000-400 cm^{-1}. FTIR shows peaks of higher intensity in the parent region of wavelength which also indicates polymerization process.

Computational study: After getting the m/z values of degraded products at different retention times from GC-MS, possible degradation mechanism is predicted [19,20]. The possible degradation path is confirmed through DFT calculations (Gaussian 16 W), by knowing their free energy, enthalpy and entropy values (unit; Hartree). The Gaussian 16 w software is used for above computational work.

RESULTS AND DISCUSSION

Paschen's curve

Paschen's law/equation the breakdown voltage, the voltage required to discharge between two electrodes in a gas, is empirically given as a function of pressure and gap length with respect to electrode shape and smoothness, separation, and the pressure of the surrounding gas, in the absence of other contributing factors such as radiation, impurities, etc. Figure 2 depicts a graph of breakdown voltage *vs.* pxd for the degradation of chloro-containing VOCs in a parallel plate DBD reactor. We initially optimized the reactor, which entails determining the voltage at which the degradation process begins and the amount of plasma generated for each VOC.

In general, at normal temperature and pressure, the breakdown voltage, Vbd, is required to generate a spark in a given gas with spherical electrode. Tips is proportional to the product of the Pressure (p) and charge surface (*i.e.* electrode) separation (d) (when mm-cm), as shown in relation (1).

$$Vbd=a \times (p \times d)/(\ln(p \times d)+b) \quad (1)$$

Wherein, a and b depend on the gas composition.

Where,

p=Pressure which is calculated from (MFC MFC)

d=Distance between the two electrode

Figure 2 illustrates Paschen's breakdown of chlorobenzene, o-dichlorobenzene, and dichloromethane. The breakdown voltages for chlorobenzene, O-dichlorobenzene, and dichloromethane are 8.0 kV, 9.2 kV, and 18.1 kV, respectively, indicating that dichloromethane requires more voltage to deteriorate due to its increased volatility. Because of the more volatile nature of the plasma, a higher voltage of up to 22.2 kV is increasingly required to sustain it. Chlorobenzene and O-dichlorobenzene undergo degradation, resulting in decreased stability and increased reactivity. The detailed mechanism of degradation is given below, and computational work is also performed to determine the viability of the degradation pathway. In addition to Paschen's curve, Figure 3 depicts the V-I figure, which demonstrates how VOC degradation fluctuates with voltage. This implies how plasma transforms from the dark discharge area.

Figure 2 depicts Paschen's split of chlorobenzene, o- to Arc discharge regions for each chlorinated VOC. Figure 3 shows a dark discharge zone, which is where plasma tends to develop. Depending on the type of VOC, the likelihood for dark discharge zones varies. After the breakdown voltage, another region appears, known as the glow discharge region. The presence of sustained plasma in this location indicates that breakdown is taking place here. As the voltage increases, so does the intensity of the plasma and the rate of breakdown. As the voltage increases, so does the density and intensity of the plasma. This results in the formation of another region known as the Arc discharge region. The arc discharge zone is the region in which non-thermal plasma becomes more intensified enhancing the temperature of electron and reactive species to higher range which creates the condition similar to thermal plasma. Beyond this region non-thermal plasma disappears.

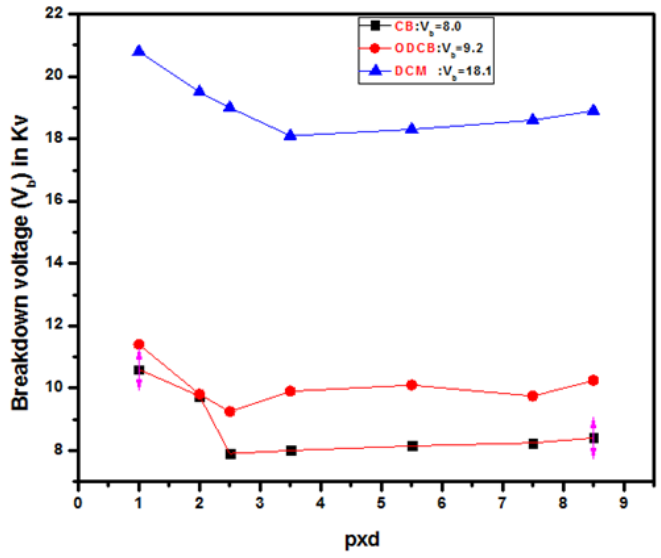

Figure 2: Paschen curve for CB, ODCB and DCM in argon plasma.

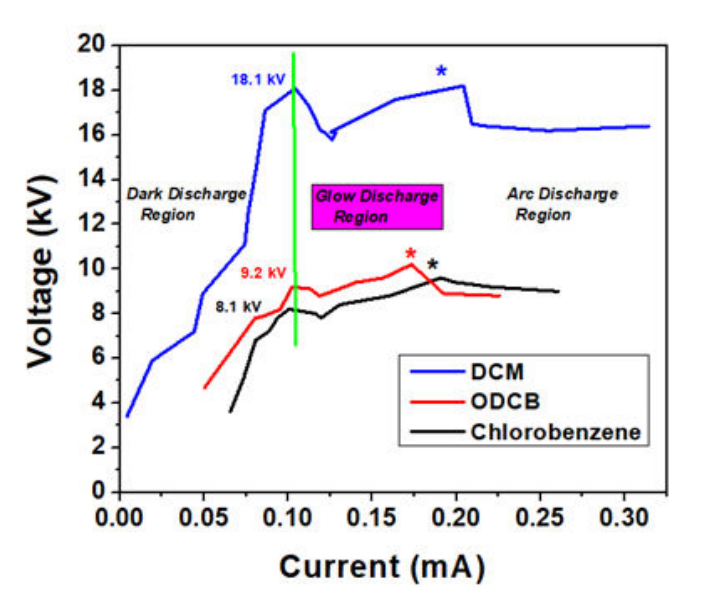

Figure 3: V-I graph of CB, ODCB and DCM.

Catalyst characterization

X-Ray Diffraction study (XRD): In this study we have taken two different oxidizing catalyst *i.e.*, CeO_2 and MnO_2. Figure 4 appears the X-ray diffraction patterns of CeO_2 and MnO_2 catalyst. The spectrograms of CeO_2 appears the characteristic peaks at 270,360 and 390. Meanwhile MnO_2 spectrogram appears at 280,380,120 and 170. In case of CeO_2 the sharpest peaks are appeared whereas no sharp peaks are appeared in case of MnO_2 and some hazy peaks are appeared. A sharper peaks indicates more crystallinity higher catalytic activity. Since CeO_2 has a larger relative permittivity than MnO_2 has the highest effect for ozone decomposition. The degradation efficiency increases in the order of CeO_2 catalyst>MnO_2 catalyst>without catalyst. Large particle size and poor specific area are two key variables that prevents metal oxides from functioning as a high-performance combustion catalyst. The catalysts interacted with highly energetic electrons that are generated during plasma reaction. On the other aspects, the presence of catalytic particles in the plasma reactor enhances the physical effect, such as an increase in electric field and the formation of more energetic electrons and reactive species, which in turn leads to plasma degradation process and helps the secondary pollutants to convert into CO_2 and lesser harmful products. The other hand, electronic energy impact on the surface of catalysts activates through the formation of these electron-hole pairs with the help of sufficient photonic energy.

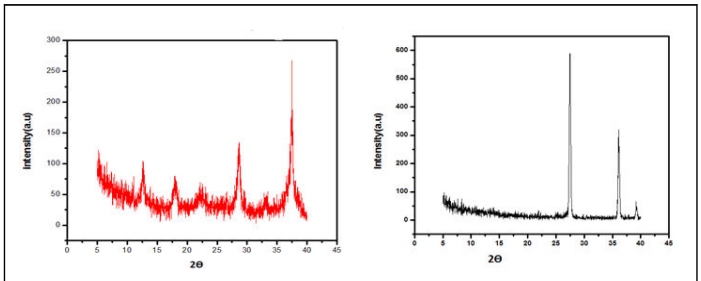

Figure 4: (a) XRD image of CeO_2 (b) MnO_2.

BET analysis: The specific area of the MnO_2 and CeO_2 are listed in Table 2. The results express that the specific area of MnO_2 and CeO_2 (before plasma treatment) are 11.86 m^2/g^{-1} and 15.26 m^2/g^{-1} respectively, indicating that both the two single oxide have relatively low specific surface area. But surface area increases after non-thermal plasma treatment and the values raises to 67.44 m^2/g^{-1} and 75.27 m^2/g^{-1}. Due to Ar plasma treatment of about 2 to 3 minutes surface etching starts and due to etching, holes are created by which specific area increases.

Table 2: BET of MnO_2 and CeO_2 catalyst.

Catalyst	Surface area (m^2/g^{-1}) before plasma treatment	Surface area (m^2/g^{-1}) after plasma treatment	Gas used	Time (in min)
MnO_2	11.86	67.44	Ar	5
CeO_2	15.26	75.27	Ar	5

Field Emission Scanning Electron Microscopy (FESEM): The morphologies of the above catalysts before plasma treatment after plasma treatment were examined by SEM. Figures 5a and 5b shows the morphological character changes of CeO_2 pre and post plasma treatment. The analysis shows that figure shows greater porosity due to ethiching process by which more number of active sites and holes are formed. Figures 5c and 5d shows morphological images of MnO_2 before and after plasma treatment. Analysis shows that after plasma treatment there is also increase of porosity, size of holes, increase in no. of active sites etc., observed in MnO_2 catalyst. But comparison study says that CeO_2 catalyst shows greater porosity, larger surface area after plasma treatment over MnO_2 catalyst.

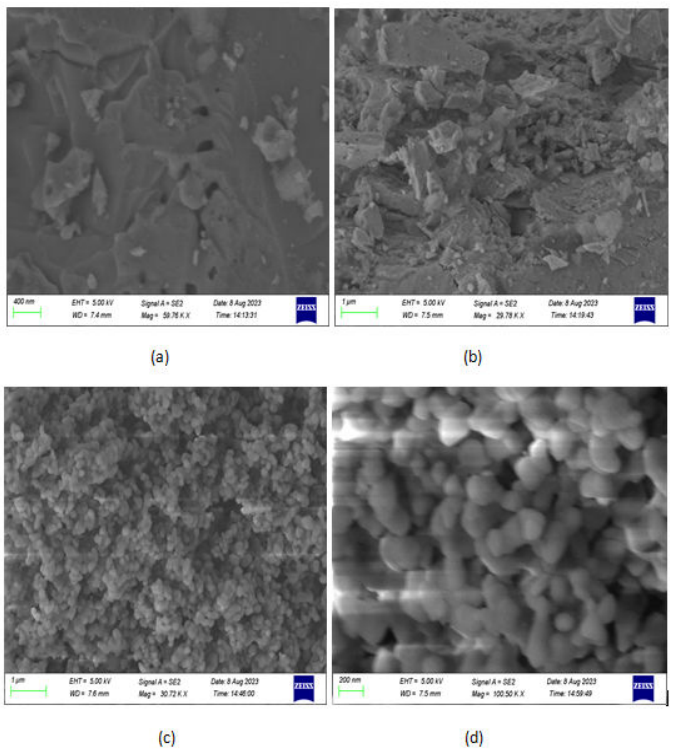

Figure 5: FESEM images of (a) CeO_2UT (b) CeO_2T (c) MnO_2UT (d) MnO_2T.

OES (Optical Emission Spectroscopy) analysis: Non-thermal plasma is characterized by the Electron Temperature (E_T) or Electron excitation Temperature (E_{exT}) and the Electron density (E_d). Optical emission spectroscopy, OES is an important technique for optical diagnostics and radicals, ions, atoms detection tool [21]. The reactive species that produced during plasma treatment with presence of catalyst (CeO_2 and MnO_2 are shown in Figure 6 below. Since all the 3 experiments with different catalysts are done at Ar environment so the key peaks of Ar (Ar I, Ar II) are found at 690 nm to 810 nm. Also we get other reactive species such as OH, CO_2, CO, CH, C_2, H, atomic O, Cl. The generated reactive species in plasma environment helps in degradation process also strengthens our predicted probable mechanism for decomposition of substrate taken into useful product and harmless product.

By analyzing the wave lengths and intensity of the emitted spectral lines, it is possible to identify the neutral particles, radicals and ions that are generates inside the plasma reactor. Previously (without catalyst work) we used normal AC power supply but in this paper pulsed AC power supply with certain frequency and duty cycle is maintained. So due to high frequency, we got high electron temperature and electron density in comparison to normal AC power supply. The electron temperature and electron density of clorobenzene, ortho-diclorobenzene and dicloromethane are identified through OES technique and are shown in Figure 6. The pressure exerted by gas has a significant impact on the electron temperature of a dielectric barrier discharge because energies that the electrons can receive in the electric field is mostly determined by their collision-free route. Higher collision leads to creates pressures that cause the electron temperature to decrease because the collision frequency of electrons increases with neutrals and ions which leads to lose energy more quickly. In contrast, the density of the plasma increases with pressure [22]. The electron mobility, which is determined by multiplying the electron drift velocity by the electric field, and the plasma density have an inverse relationship [23]. Although the average electron density largely depends on the operating mode, we could see that as the duty cycle of the pulse is reduced, the average electron temperature increases quickly irrespective of the operating mode.

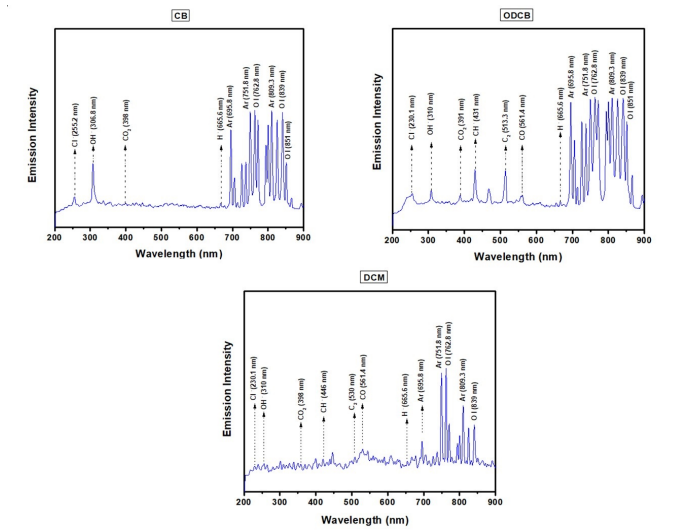

Figure 6: OES spectra of NTP treated CB, ODCB and DCM.

Electron temperature and electron density: Electron temperature and electron density (electrons are generated and participated in degradation process) both are important plasma parameters in abatement process. By using the line intensity ratio approach, which is derived from the Boltzmann and Saha equation, electron temperature and density are determined [24,25]. The above experiment has shown that with increase in applied voltage, electron temperature and density both rise, demonstrating an increase in ionization. ODCB has stable resonating structure and highest bond energy compared to other two Vocs that's why it needs greater energy (electron temperature) for degradation in plasma process. CB possess stable resonating structure as it is an aromatic compound that's why it needs greater electron temperature compared to DCM., similar case happens for electron density calculation but Ar shows highest electron density value because of higher percentage of concentration (Figure 7).

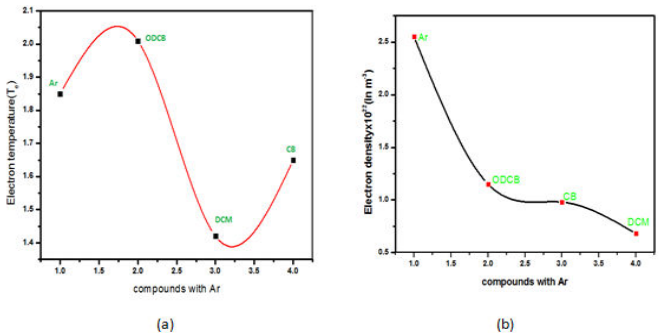

Figure 7: Variation of electron temperature (a) and electron density (b) for different VOCs.

Effect of different catalyst on pollutants: In this work, we have taken two oxidizing catalyst (oxidizing catalyst shows greater and effective catalytic activity compared to reducing catalyst). We choose two catalyst like CeO_2 and MnO_2. Since CeO_2 has a larger relative permittivity than MnO_2, so it shows greater degradation efficiency and MnO_2 has the highest effect for ozone decomposition. The removal efficiency increased significantly with catalyst in comparison to without catalyst. The degradation efficiency increased in the order of: CeO_2 catalyst>MnO_2 catalyst>without catalyst.

The above catalysts collides with energetic electrons that are generated during the non-thermal plasma reaction. On the one hand, the presence of catalytic species in the plasma reactor was critical in causing the physical effects, like an increase in the electric field and the formation of more energetic electrons, radicals and excited species, which in turn leads to speed up the chemical processes and degrade the pollutants into lesser harmful products such as CO_2 and other hydrocarbons [26-31].

By plasma treating one on the other at the same retention time, the decomposition efficiency of chlorobenzene, ortho-diclorobenzene and dicloromethane before and after non-thermal plasma treatment is analysed in GCMS. The effect of Specific Input Energy (SIE) value with respect to different flow rate was also investigated. The flow rate value w.r.t SIE value was shown in Figure 8 and with respect to efficiency percentage of chlorobenzene, ortho-diclorobenzene and dicloromethane was shown in Figure 9. With increase of flow rate the SIE value decreases. Compared to chlorobenzene and ortho-dichlorobenzene, dichloromethane has a higher input energy value. This could be as a result of dichlromethane's greater bond energy, which, in contrast to chlorobenzene and orthodichlorobenzene, requires high voltage to decay. Chlorobenzene has a greater input energy value than orthodichlorobenzene because it degrades more quickly even using without catalyst. By knowing the m/z values of peaks in chromatograms possible products are established. From the Figure 10 the maximum decomposition efficiency of clorobenzene, ortho-diclorobenzene, dicloromethane are 93%, 91% and 97.8% respectively.

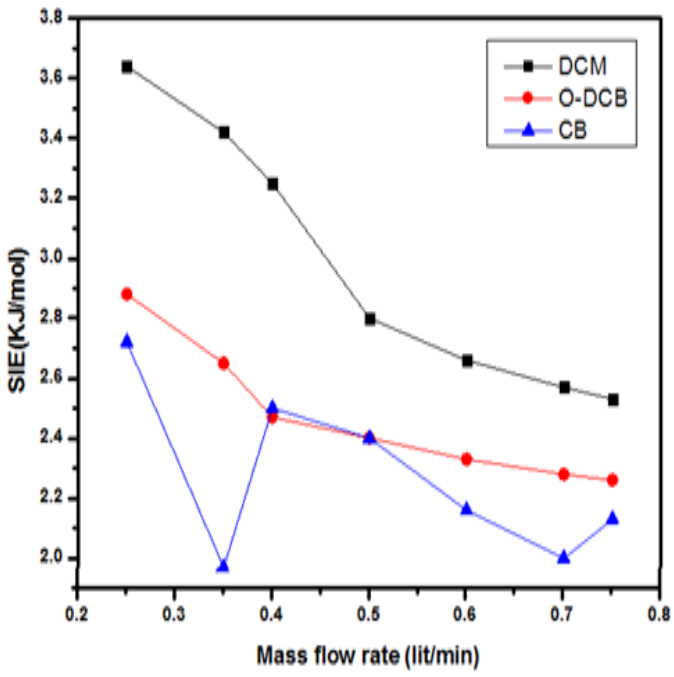

Figure 8: Effect of mass flow rate on SIE value.

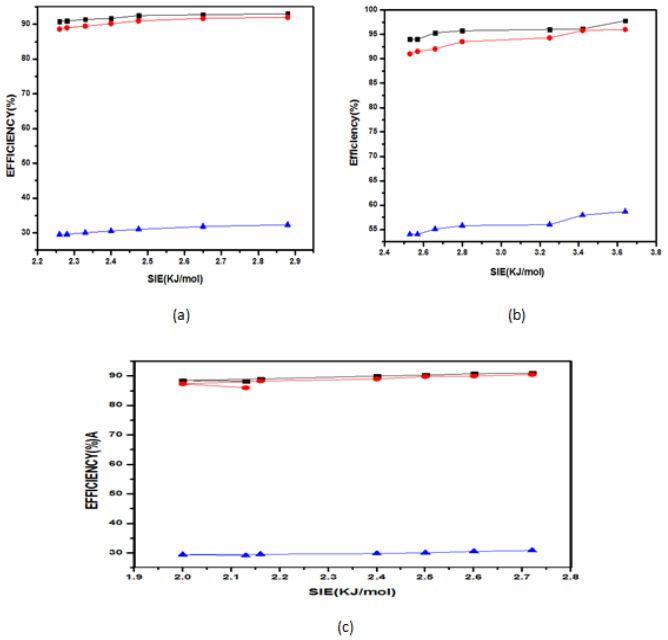

Figure 9: Plot of SIE w.r.t. removal efficiency (%) a) CB b) DCM c) ODCB.

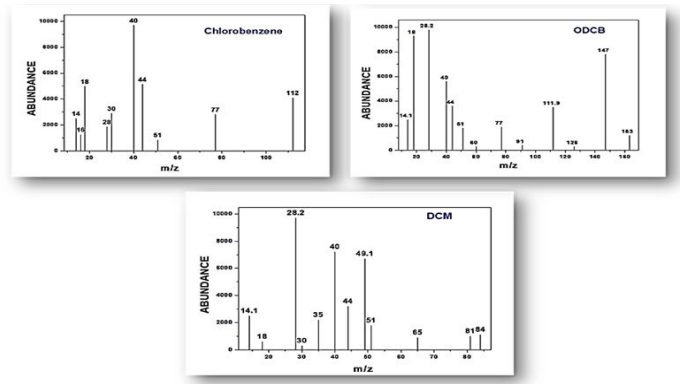

Figure 10: Plot of abundance w.r.t. fragmented mass value.

The GCMS plot shows different kinds of fragmented products are formed at different retention time which is listed below in Table 1. From the above efficiency plot we found efficiency percentage of above VOCs using catalysts and a comparision plot has been found. From above the graphs we got the percentage of efficiency without catalyst for Dichloromethane and ortho-dichlorobenzene are 58.67% and 30% by similar procedure which is employed for efficiency calculation for chlorobenzene (32.3%). Using catalyst the degradation efficiency of above VOC s increases to 93% for chlorobenzene, 91% for ortho dichlorobenzene and 97.8% for dichloromethane. Above VOCs shows greater degradation efficiency in presence of CeO_2 as compared to MnO_2. From the above plot we got higher percentage of efficiency in case of dichloromethane compared to other two VOCs probably due to its greater volatile character and high vapour pressure as well.

Due to conjugation with π-electrons of the ring in an aromatic ring helps C-Cl bond acquires a partial double bond character due to resonance which leads to make bond cleavage difficult. Another reason due to hybridization, in case of chlorobenzene and ortho-dichlorobenzene the sp^2 hybridized carbon with a greater s-character can hold the electron pair of C-Cl bond more tightly than sp^3 hybridized carbon in dichloro methane with less s-character which leads C-Cl bond weak. But if we compare the degradadation efficiency of chlorobenzene and ortho-dichlorobenzene, chlorobenzene shows higher efficiency compared to ortho-dichlorobenzene due to presence of single chlorine group. As we know chlorine shows electron withdrawing effect that means it can withdraws electron from benzene ring easily. In case of chlorobenzene presence of one chloro group enhances its degradation efficiency as compared to ortho dichlorobenzene due to its C-Cl bond breaking energy. In other words C-Cl bond can easily break in case in chlorobenzene as compared to orthodichlorobenzene which leads to enhance the reactivity of ring and for which efficiency increase. Interesting fact is that there is not so much difference in percentage of efficiency between them only because of their energy difference of C-Cl bond. In general aliphatic chloro containing organic compounds possess greater reactivity. It may be due to its hybridization and absence of aromatic ring. The probable reaction pathways are given below and further to check the feasibility of that reaction pathway computation work has been done. Different fragmented products are identified by GC-MS for different VOCs which are listed below in the form of Table 3 with different retention time. In general the fragmented products which are produced completely mention in the reaction mechanism pathway which are given below.

Three distinct schemes are provided for the potential paths for the abatement of chlorobenzene, orthodichlorobenzene and dichloromethane based on the organic intermediates found by OES, GC, GCMS, and FTIR (Figure 11 and Table 3).

Degradation mechanism

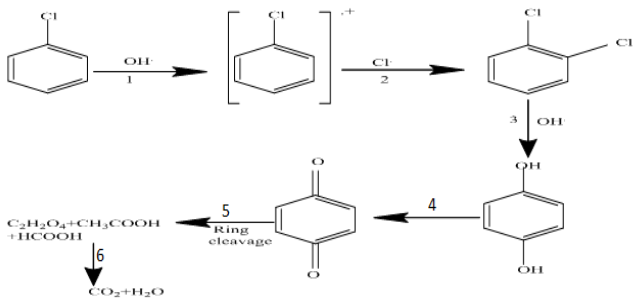

Figure 11: Probable reaction pathways of chlorobenzene decomposition.

Table 3: Theoretical calculations of chlorobenzene decomposition.

No. of steps	ΔG	ΔH	ΔS
Step-1	-0.138	-0.127	24.001
Step-2	-0.229	-0.217	27.182
Step-3	-0.556	-0.5532	+4.026
Step-4	-0.646	-0.641	+1.467
Step-5	-0.642	-0.625	+35.461
Step-6	-0.078	-0.077	1.272

In the 1st step of degradation process the chlorobenzene molecule and the excited species along with carrier gas initially collides to generate the chlorobenzene cation/radical and also produces chlorine radical. In the 2nd step generated chlorine radicals reacts to form dichlorobenzene and less harmful products. Because of the oxidizing catalyst and presence of some hydroxyl radicals, chlorobenzene can rapidly transform into the similarly dangerous Benzoquinone and hydroquinone in 3rd and 4th step [32]. Ring cleavage occurs in step 5 produces some acidic polymeric products and in the final step of the mechanism produces useful hydrocarbons and water particles. Despite the fact that plasma is an electron-induced process, phenol and hydroquinone can also decompose into less dangerous substances like CO_2 and CO, water molecule and other useful hydrocarbons. As in this plasma degradation process, some oxidizing catalysts are used for speed up the reaction, there is no such things noticed only the reaction pathway in addition to that some energy factor changes. In the field of computational chemistry, Gaussian 16 W is a program that is utilized to calculate bond energy in terms of Gibbs free energy (ΔG), enthalpy (ΔH), and entropy (S). The proposed probable process is determined to be thermodynamically feasible. According to the thermodynamic principle, each spontaneous reaction should have a negative Gibbs free energy and enthalpy. Gaussian 16 W software followed by DFT method is used to determine these thermodynamic parameters. Since the molecule has valence and core electrons, the fundamental set is 6-311G with B-3LYP. At first we optimized each compound and then we calculate their frequency values. All of the aforementioned expected stages are feasible (Figure 12 and Table 4).

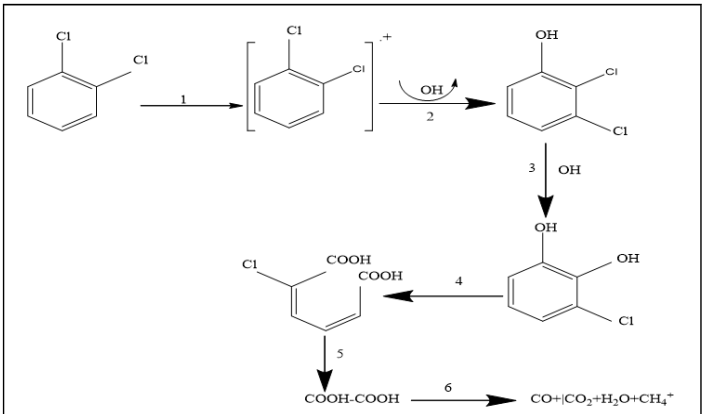

Figure 12: Probable reaction pathways of ortho-dichloro benzene decomposition mechanism.

Table 4: Calculations on the theoretical breakdown of dichlorobenzene.

No. of steps	ΔG	ΔH	ΔS
Step-1	-90.36	-89.01	45.32
Step-2	-96.3	-96.1	25.5
Step-3	-108.35	-107.35	52.25
Step-4	-125.53	-124.38	38.3
Step-5	-128.39	-127.48	35.2
Step-6	-132.99	-131.36	40.19

In comparison to chlorobenzene, dichlorobenzene shows greater reactivity towards for degradation due to formation of multiple products and generates high energy. Step-1 shows dichlorobenzene molecule interacts with excited argon gas and with excited electron to form the respective ions and chlorine radicals and excited electrons. in the 2nd step interactions of hydroxyl ion and electrons leads to form 1-Hydroxy,2,3-Dichlorobenzene, again collision with same ions to form 1,2-Hydroxy,3-Chlorobenzene products which are again decomposed to lesser harmful products (Figure 13 and Table 5).

Mechanism 1

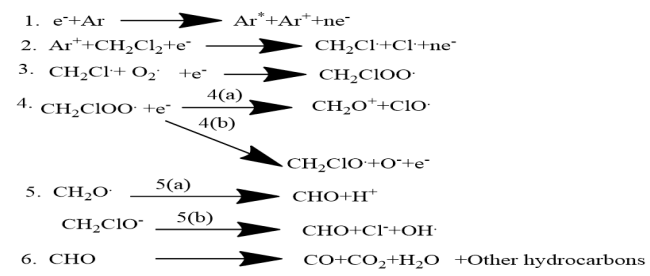

Figure 13: Probable reaction pathways of dichloro methane decomposition.

Table 5: Calculations on the theoretical breakdown of dichloromethane.

No. of steps	ΔG	ΔH	ΔS
Step-1	-0.527	-0.51	37.1
Step-2	-153.26	-153.1	15.13
Step-3	-150.275	-150.342	14.112
Step-4(a)	-150.56	-150.98	16.89
Step-4(b)	-75.05	-74.3	3.95
Step-5(a)	-90.3	-91.35	1.88
Step-5(b)	-101.23	-102.33	3.35
Step-6	-120.52	-120.56	8.45

Dichloromethane shows greater reactivity compared to other VOCs like chlorobenzene and orthodichlorobenzene due to easy rupturing/breaking of bonds. As it possesses higher reactivity and more hazardous compared to others, it produces secondary pollutants as well as hazardous substances. On this aspect it shows two types of pathways for degradation process which is shown in mechanism 1 and 2. In mechanism 1 degradation completes within 8 steps. Initial three steps show the primary plasma reaction for the production of CH_2ClOO. But at the 4th step it splits up into two processes and step 4(a) shows greater spontaneity due to high negative free energy values. In step-4 production of secondary pollutants like CH_2O+, ClO-, CH_2ClO. Are produced which are harmful substances (by non-thermal ionic collision reaction in plasma reactor). In step 5 the secondary pollutants are split up into Aldehyde and some bi-products. Between two sub steps of 5, step 5(b) shows greater spontaneity due to greater negative Gibbs free energy value. In the final step aldehyde degraded into less harmful products (Figure 14 and Table 6).

Mechanism 2

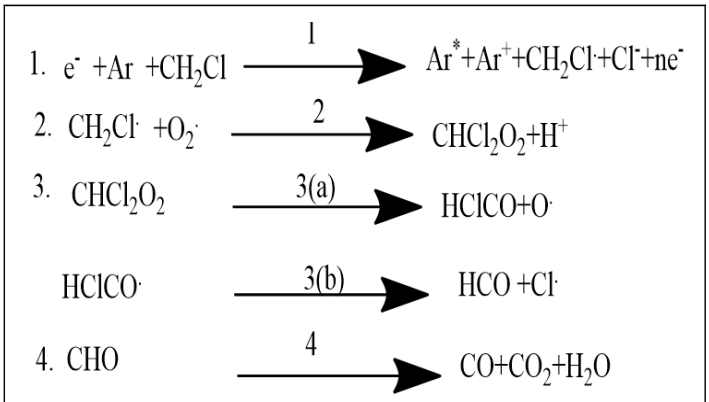

Figure 14: Dichloromethane takes 4 steps to complete degradation.

Table 6: Calculations of theoretical values following the breakdown of dichloromethane.

No. of steps	ΔG	ΔH	ΔS
Step-1	-80.55	-81.33	30.25
Step-2	-91.33	-90.34	25.33

Step-3(a)	-95.48	-94.38	20.39
Step-3(b)	-96.39	-95.48	21.43
Step-4	-102.33	-103.36	30.33

In mechanism 2, dichloromethane takes 4 steps to complete degradation. In the first step dichloromethane molecule collides with argon gas and energized electron to form excited argon gas, chlorine radicals and dichloromethane ions. In the 2nd step oxygen induced plasma reaction occurred and one secondary pollutant produced. In the very next step $CHCl_2O_2$ degraded into two different types of secondary harmful products. Step 3(b) shows greater spontaneity towards product formation due to high negative value of Gibbs free energy value. Between above two possible degradation mechanism, 1st one shows greater feasibility compared to 2nd one due to high negative values and lesser percentage formation of secondary pollutants.

Gas Chromatography (GC)

The analysis of peaks that found in GC in chromatogram is mainly CO_2, CO, acetylene, ethane, methane and other hydrocarbons. But for this work, we only calculated the yield percentage of CO_2 and CO which are shown in Figure 15. It is observed that for chlorobenzene, orthodichlorobenzene and dichloromethane all the peaks of CO_2, CO peaks are found. Since we employed oxidizing catalysts, the bulk of the byproducts that we previously detected are converted to CO_2, CO, and some other less harmful compounds.

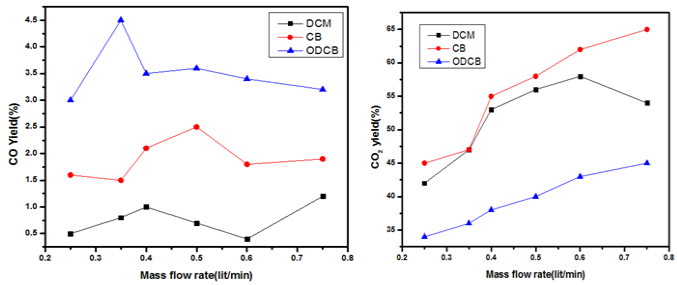

Figure 15: Yield percentage of CO_2 and CO with mass flow rate in presence of catalyst.

In comparison to toluene and dichloromethane and orthodichlorobenzene, we discover that chlorobenzene has a higher yield percentage of CO_2. The quantity of CO_2 influences the number of hydrocarbons and other byproducts. Dichloromethane and chlorobenzene exhibit higher output percentages of CO_2 than orthodichlorobenzene. By employing a catalyst, the yield percentage of CO_2 in chlorobenzene and dichloromethane is increasing from 35% to ~ 65%. And it rises from ~25% to ~43% in the case of benzene. Due to the use of catalyst, in every instance, we discover a very low CO yield percentage. The yield percentage of CO in DCM and CB is reducing similarly utilizing catalyst, from ~2.5% to ~0.5% and from ~4.5% to ~3% in the case of benzene.

FTIR analysis

After plasma treatment we noticed some particles are deposited on the glass surface of the DBD reactor for each substrate like chlorobenzene, ortho-dichlorobenzene and Dichloromethane. These are washed and collected with ethanol and then FTIR study is done. The deposited products are analysed through GCMS and to confirm type of functional groups are present. In case of chlorobenzene spectra are analysed and compared pure CB with deposited product of CB. In case of pure chlorobenzene (before plasma treatment) several peaks are observed at 3068.39 cm^{-1} due to C-H stretching in alkene, 1936.44 cm^{-1} due to C-H bending in aromatic ring, 734.32 cm^{-1} is due to C-Cl bond in mono substituted aromatic alkyl halide. Whereas in case of another line which shows some new peaks at 3448.35 cm^{-1} due to -OH group, 1634.05 cm^{-1} is due to C=O group and 1035.85cm^{-1} due to C-O stretching frequency and some peaks are disappeared due to decomposition of that substance and peaks are disappeared and merged which shows some hydrocarbon products are formed and some polymeric materials also which are deposited on the dielectric materials and are analysed through GC and GCMS. Similarly in case of ODCB as like as CB similar peaks are observed. But new peaks are observed at 2350 cm^{-1} due to C=O stretching frequency in carbon dioxide and an important peak is also formed at 1760 cm^{-1} which confirms presence of C=O group in carboxylic acid group. And other peaks are disappeared due to degradation by plasma and red line becomes straight may be due to polymerization. If we look at the FTIR spectra of DCM we found that more peaks are disappeared and lines are become more straight which confirms more degradation and peaks at 1630.92 cm^{-1} and 1380.78 cm^{-1} are due to presence of C=O group in carbon dioxide and C=O group in aldehydic group (Figure 16) [33-37].

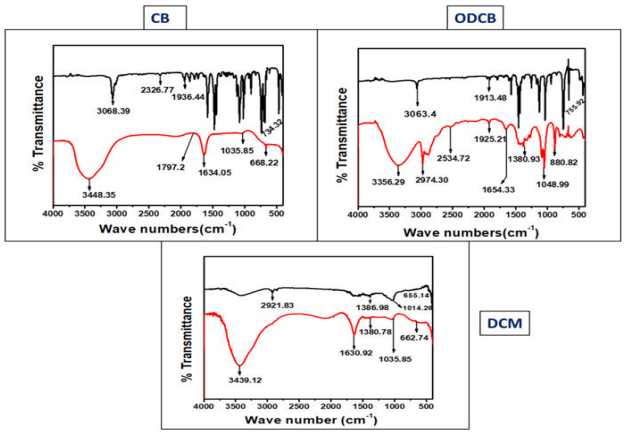

Figure 16: FTIR spectra of CB, ODCB, DCM of pure and plasma treated sample.

The ozone peak, which is at 1124 cm^{-1}, can also be found here. We found very less percent of Mn-O/Ti-OH and Ti-O peaks at 523 cm^{-1} and 768 cm^{-1}, respectively, which may be due to the use of catalyst. All of these peaks that were discovered following plasma treatment provide a solid demonstration of the mechanism that we hypothesized.

CONCLUSION

In this work we have considered hazardous chloro containing aromatic and aliphatic compounds such as chlorobenzene, O-dichlorobenzene and dichloromethane for abatement. These VOCs are decomposed through Dielectric Barrier Discharge (DBD) plasma mediated technique at atmospheric pressure in presence of argon as a carrier gas and their characteristic effects were also studied. The by-products those were deposited on dielectric surface after plasma treatment was analyzed by different analytical techniques like as GC, GC-MS, FTIR and OES. VOCs degradation to CO, CO_2 and CH_4 was confirmed through GC and GC-MS analysis. Among all Dichloromethane possess highest degradation efficiency (97.8%) compared to chlorobenzene (93%) and dichlorobenzene (91%). OES gives the radicals are generated in the plasma reactor which are also take part in the degradation process using which probable mechanism has been predicted. Furthermore, the probable degradation pathway for the degradation of the above mentioned VOCs has been deciphered and the most feasible path was suggested through theoretical calculations. The probable pathway predicted are energetically supported by Gaussion16 W using DFT calculations which is proved from verification of OES spectra and GC-MS, GC, FTIR data analysis. It is expected that varying pulsed time, frequency, and voltage and flow rate along with use of suitable catalyst will open a more efficient pollutant abatement methodology for better environment.

REFERENCES

1. Chao CY, Kwong CW, Hui KS. Potential use of a combined ozone and zeolite system for gaseous toluene elimination. J Hazard Mater. 2007;143(1-2):118-127.
2. Choi PG, Ohno T, Masui T, Imanaka N. Catalytic liquid phase oxidation of acetaldehyde to acetic acid over a Pt/CeO_2–ZrO_2–SnO_2/γ-alumina catalyst. J Environ Sci. 2015;36:63-66.
3. Schmid S, Jecklin MC, Zenobi R. Degradation of volatile organic compounds in a non-thermal plasma air purifier. Chemosphere. 2010;79(2):124-130.
4. Priya VS, Philip L. Treatment of volatile organic compounds in pharmaceutical wastewater using submerged aerated biological filter. Chem Eng J. 2015;266:309-319.
5. Whalley LK, Slater EJ, Woodward-Massey R, Ye C, Lee JD, Squires F, et al. Evaluating the sensitivity of radical chemistry and ozone formation to ambient VOCs and NOx in Beijing. Atmos Chem Phys. 2021;21(3):2125-2147.
6. Lin F, Zhang Z, Li N, Yan B, He C, Hao Z, et al. How to achieve complete elimination of Cl-VOCs: A critical review on byproducts formation and inhibition strategies during catalytic oxidation. Chem Eng J. 2021;404:126534.
7. Choi MS, Qiu X, Zhang J, Wang S, Li X, Sun Y, et al. Study of secondary organic aerosol formation from chlorine radical-initiated oxidation of volatile organic compounds in a polluted atmosphere using a 3D chemical transport model. Environ Sci Technol. 2020;54(21):13409-13418.
8. Vilve M, Vilhunen S, Vepsalainen M, Kurniawan TA, Lehtonen N, Isomaki H, et al. Degradation of 1, 2-dichloroethane from wash water of ion-exchange resin using Fenton's oxidation. Environ Sci Pollut Res. 2010;17:875-884.
9. Che H, Bae S, Lee W. Degradation of trichloroethylene by Fenton reaction in pyrite suspension. J Hazard Mater. 2011;185(2-3): 1355-1361.
10. Che H, Lee W. Selective redox degradation of chlorinated aliphatic compounds by Fenton reaction in pyrite suspension. Chemosphere. 2011;82(8):1103-1108.
11. Munoz M, de Pedro ZM, Casas JA, Rodriguez JJ. Assessment of the generation of chlorinated byproducts upon Fenton-like oxidation of chlorophenols at different conditions. J Hazard Mater. 2011;190(1-3):993-1000.
12. Karci A, Arslan-Alaton I, Olmez-Hanci T, Bekbolet M. Transformation of 2,4-ichlorophenol by H_2O_2/UV-C, Fenton and photo-Fenton processes: Oxidation products and toxicity evolution. J Photochem Photobiol A: Chemistry. 2012;230(1):65-73.
13. Li R, Jin X, Megharaj M, Naidu R, Chen Z. Heterogeneous Fenton oxidation of 2,4-dichlorophenol using iron-based nanoparticles and persulfate system. Chem Eng J. 2015;264:587-594.
14. Chen H, Mu Y, Shao Y, Chansai S, Xu S, Stere CE, et al. Coupling non-thermal plasma with Ni catalysts supported on BETA zeolite for catalytic CO_2 methanation. Catal Sci Technol 2019;9(15): 4135-4145.
15. Tang X, Feng F, Ye L, Zhang X, Huang Y, Liu Z, et al. Removal of dilute VOCs in air by post-plasma catalysis over Ag-based composite oxide catalysts. Catal Today. 2013;211:39-43.
16. Xiao G, Xu W, Wu R, Ni M, Du C, Gao X, et al. Non-thermal plasmas for VOCs abatement. Plasma Chem Plasma Process. 2014;34:1033-1065.
17. Adelodun AA. Influence of operation conditions on the performance of non-thermal plasma technology for VOC pollution control. J Ind Eng Chem. 2020;92:41-55.
18. Donnelly VM. Plasma electron temperatures and electron energy distributions measured by trace rare gases optical emission spectroscopy. J Phys D: Appl Phys. 2004;37(19):R217.
19. Mohanty S, Das SP. DBD non-thermal plasma for decomposition of DBD non-thermal Plasma for decomposition of volatile organic compounds. Int J Sci Res. 2014;3:1360-1362.
20. Gushchin AA, Grinevich VI, Kozlov A, Kvitkova EY, Shutov DA, Rybkin V. Destruction of 2,4-dichlorophenol in an atmospheric pressure dielectric barrier discharge in oxygen. Plasma Chem Plasma Process. 2017;37:1331-1341.
21. Cheng Z, Qu M, Chen D, Chen J, Yu J, Zhang S, et al. Mechanisms of active substances in a dielectric barrier discharge reactor: species determination, interaction analysis, and contribution to chlorobenzene removal. Environ Sci Technol. 2021;55(6): 3956-3966.
22. Zhu R, Mao Y, Jiang L, Chen J. Performance of chlorobenzene removal in a nonthermal plasma catalysis reactor and evaluation of its byproducts. Chem Eng J. 2015;279:463-471.
23. Zhou W, Ye Z, Nikiforov A, Chen J, Wang J, Zhao L, et al. The influence of relative humidity on double dielectric barrier discharge plasma for chlorobenzene removal. J Clean Prod. 2021;288:125502.
24. Zhao J, Xi W, Tu C, Dai Q, Wang X. Catalytic oxidation of chlorinated VOCs over Ru/TixSn1-x catalysts. Appl Catal B: Environ. 2020;263:118237.

25. Valdes H, Riquelme AL, Solar VA, Azzolina-Jury F, Thibault-Starzyk F. Removal of chlorinated volatile organic compounds onto natural and Cu-modified zeolite: The role of chemical surface characteristics in the adsorption mechanism. Sep Purif Technol. 2021;258:118080.
26. Kozicki M, Guzik K. Comparison of VOC emissions produced by different types of adhesives based on test chambers. Materials. 2021;14(8):1924.
27. Cheng ZW, Zhang LL, Chen JM, Yu JM, Gao ZL, Jiang YF. Treatment of gaseous alpha-pinene by a combined system containing photo oxidation and aerobic bio-trickling filtration. J Hazard Mater. 2011;192(3):1650-1658.
28. Karuppiah J, Reddy MKP, Reddy LE, Subrahmanyam C. Catalytic non-thermal plasma reactor for decomposition of dilute chlorobenzene. Plasma Process Polym. 2013;10(12):1074-1080.
29. Penetrante BM, Schultheis SE. Non-thermal plasma techniques for pollution control: Part b: Electron beam and electrical discharge processing. Springer Science and Business Media. 2013.
30. Parr RG, Gadre SR, Bartolotti LJ. Local density functional theory of atoms and molecules. Proc Natl Acad Sci. 1979;76(6):2522-2526.
31. Huang RJ, Zhang Y, Bozzetti C, Ho KF, Cao JJ, Han Y, et al. High secondary aerosol contribution to particulate pollution during haze events in China. Nature. 2014;514(7521):218-222.
32. Yang P, Zuo S, Shi Z, Tao F, Zhou R. Elimination of 1, 2-dichloroethane over (Ce, Cr) xO_2/MOy catalysts (M=Ti, V, Nb, Mo, W and La). Appl Cata B: Environ. 2016;191:53-61.
33. Abedi K, Ghorbani-Shahna F, Jaleh B, Bahrami A, Yarahmadi R, Haddadi R, et al. Decomposition of Chlorinated Volatile Organic Compounds (CVOCs) using NTP coupled with TiO_2/GAC, ZnO/GAC, and TiO_2–ZnO/GAC in a plasma-assisted catalysis system. J Electrostat. 2015;73:80-88.
34. Belaissaoui B, Le Moullec Y, Favre E. Energy efficiency of a hybrid membrane/condensation process for VOC (Volatile Organic Compounds) recovery from air: A generic approach. Energy. 2016;95:291-302.
35. Bloemen HJ, Burn J. Chemistry and analysis of volatile organic compounds in the environment. Springer, London. 2012.
36. Zhou W, Ye Z, Nikiforov A, Chen J, Wang J, Zhao L, et al. The influence of relative humidity on double dielectric barrier discharge plasma for chlorobenzene removal. J Clean Prod. 2021;288:125502.
37. Wallis AE, Whitehead JC, Zhang K. The removal of dichloromethane from atmospheric pressure nitrogen gas streams using plasma assisted catalysis. Appl Cata B: Environ. 2007;74(1-2):111-116.